Received: 19 November 2023 | Revised: 2 April 2024 | Accepted: 11 April 2024

DOI: 10.1096/fj.202302375R

RESEARCH ARTICLE

The FASEB Journal

CDK9 inhibition activates innate immune response through viral mimicry

Shivani Yalala[1] | **Aishwarya Gondane**[1] | **Ninu Poulose**[2] | **Jing Liang**[1] | **Ian G. Mills**[2] | **Harri M. Itkonen**[1]

[1]Department of Biochemistry and Developmental Biology, Faculty of Medicine, University of Helsinki, Helsinki, Finland

[2]Nuffield Department of Surgical Sciences, University of Oxford, John Radcliffe Hospital, Oxford, UK

Correspondence
Harri M. Itkonen, Department of Biochemistry and Developmental Biology, Faculty of Medicine, University of Helsinki, Haartmaninkatu 8, Helsinki 00014, Finland.
Email: harri.itkonen@helsinki.fi

Funding information
Opetushallitus (EDUFI); Magnus Ehrnroothin Säätiö (Magnus Ehrnrooth Foundation); Rosetrees Trust (Rosetrees), Grant/Award Number: PGL21/10171 and Seedcorn2021\100216; Maud Kuistila Memorial Foundation; John Black Charitable Foundation (JBCF); Prostate Cancer UK (Prostate Cancer); Research Council of Finland (AKA), Grant/Award Number: 331324, 358112 and 335902; The Jenny and Antti Wihuri Foundation; Sigrid Juselius Foundation

Abstract

Cancer cells frequently exhibit hyperactivation of transcription, which can lead to increased sensitivity to compounds targeting the transcriptional kinases, in particular CDK9. However, mechanistic details of CDK9 inhibition-induced cancer cell-selective anti-proliferative effects remain largely unknown. Here, we discover that CDK9 inhibition activates the innate immune response through viral mimicry in cancer cells. In MYC over-expressing prostate cancer cells, CDK9 inhibition leads to the gross accumulation of mis-spliced RNA. Double-stranded RNA (dsRNA)-activated kinase can recognize these mis-spliced RNAs, and we show that the activity of this kinase is required for the CDK9 inhibitor-induced anti-proliferative effects. Using time-resolved transcriptional profiling (SLAM-seq), targeted proteomics, and ChIP-seq, we show that, similar to viral infection, CDK9 inhibition significantly suppresses transcription of most genes but allows selective transcription and translation of cytokines related to the innate immune response. In particular, CDK9 inhibition activates NFκB-driven cytokine signaling at the transcriptional and secretome levels. The transcriptional signature induced by CDK9 inhibition identifies prostate cancers with a high level of genome instability. We propose that it is possible to induce similar effects in patients using CDK9 inhibition, which, we show, causes DNA damage *in vitro*. In the future, it is important to establish whether CDK9 inhibitors can potentiate the effects of immunotherapy against late-stage prostate cancer, a currently lethal disease.

Abbreviations: AR, androgen receptor; ATCC, American tissue culture collection; BCA assay, bicinchoninic acid assay; CDK9, cyclin-dependent kinase 9; CLK3, CDC-Like Kinase 3; CSS, charcoal-stripped FBS; CXCL10, C-X-C Motif Chemokine Ligand 10; dsRNA, double-stranded RNA; DUNK, Digital Unmasking of Nucleotide conversion-containing k-mers; EIF2AK2, protein kinase R; FBS, fetal bovine serum; GSEA, gene set enrichment analysis; IL8, C-X-C Motif Chemokine Ligand 8; IR, intron retention; KLK3, kallikrein related peptidase 3; MAVS, mitochondrial antiviral signaling; mTOR, mechanistic target of rapamycin kinase; NFkB, nuclear factor kappa-B; OGT, O-Linked N-Acetylglucosamine (GlcNAc) Transferase; PBS, phosphate-buffered saline; PKR, protein kinase R; PRO-seq, precision nuclear run-on sequencing; RELA, RELA Proto-Oncogene; SLAM-seq, thiol(SH)-linked alkylation for the metabolic sequencing of RNA; TBK1, TANK-binding kinase 1; TNFα, tumor necrosis factor alpha; TT-seq, transient transcriptome sequencing; WGA, wheat germ agglutinin.

This is an open access article under the terms of the Creative Commons Attribution License, which permits use, distribution and reproduction in any medium, provided the original work is properly cited.
© 2024 The Authors. *The FASEB Journal* published by Wiley Periodicals LLC on behalf of Federation of American Societies for Experimental Biology.

KEYWORDS
cyclin-dependent kinase 9, cytokines, innate immune response, prostate cancer, SLAM-seq, splicing

1 | INTRODUCTION

Prostate cancer is the most common cancer in men, and it is one of the leading causes of cancer-related deaths.[1,2] Prostate cancer is characterized by elevated activity of a transcription factor, androgen receptor (AR), and hence the mainstream treatment against this disease is anti-androgen therapy. However, in many cases, resistance against the AR-targeted therapies arises, and the pro-proliferative transcriptional programs are restored, which allows the cancer cells to proliferate despite the presence of the therapy.

AR functions as a general suppressor of the immune system. Of particular interest for cancer research, AR governs the expression of the immune-suppressive program to promote the survival of sperm in the female reproductive tract.[3–5] We have previously performed AR ChIP-seq experiments on both normal prostate tissue and prostate cancer patient samples, and shown that over half of the AR binding sites found in the normal prostate tissue are also present in the cancer samples.[6] In general, prostate tumors are immunologically cold,[7] and the ability to render prostate cancer cells more visible to the immune system has significant translational value.

Alternative splicing has profound effects on transcriptional diversity, allowing cells to rapidly adapt to environmental and intrinsic stress. Alternative splicing can also be therapeutically hyperactivated in cancer cells to attract the immune system to eliminate these cells.[8–10] In breast cancer, intron retention (IR) is significantly boosted by MYC overexpression or spliceosome inhibition.[11] IR refers to a situation where one of the introns is kept in the otherwise processed mRNA, and this mis-spliced mRNA is transported to cytosol.[8,11] Consequently, certain treatments applied to MYC-driven cancers lead to excessive accumulation of the IR mRNAs, some of which form double-stranded RNAs, and ultimately, activation of the innate immune response-dependent elimination of the cancer cells.[11] Essentially, targeting the core splicing machinery triggers selective effects in the cancer cells, which exhibit high levels of transcription.

All cells depend on transcription, but an increased transcription rate is characteristic of cancer cells. A cancer cell-selective increase in transcription burdens the spliceosome machinery, and intron retention can be seen as a manifestation of this stress.[12,13] Cyclin-dependent kinase 9 (CDK9) phosphorylates RNA polymerase II to recruit the appropriate splicing machinery to the polymerase and to allow productive transcription elongation of the protein-encoding part of the genome.[14] Accordingly, we have shown that CDK9 inhibition causes splicing defects primarily by increasing intron retention.[15]

Dysregulated alternative splicing and aberrant intron retention are some of the features of late-stage, lethal prostate cancer but are not sufficient to activate the innate immune response.[16] Interestingly, analogous to breast cancer, MYC is a master regulator of alternative splicing in prostate cancer cells as well.[17] As a result, we hypothesize that particular treatments will boost immunogenicity and result in effective immune-dependent clearance/surveillance of prostate cancer cells with hyperactivated MYC; CDK9 inhibitors are an excellent candidate to achieve this.

Decreased global transcription has been postulated as the major anti-tumor effect of CDK9 inhibitors. Although transcription is a ubiquitous cellular process, phase I–III clinical trials have validated small-molecule inhibitors against CDK9 as potential cancer therapy.[12,18,19] The mRNAs encoding pro-proliferative and anti-apoptotic proteins have short half-lives, and high levels of transcription are required for their robust expression.[20] Since all cells depend on active transcription, cancer cells are likely to have additional features that explain their addiction to high CDK9 activity.

Here, we show that inhibition of CDK9 activity causes anti-proliferative effects in prostate cancer cells by activating the innate immune response through the double-stranded RNA sensor PKR (protein kinase R). We use time-resolved RNA-seq (SLAM-seq) and cytokine profiling to show that targeting CDK9 activates immunogenic signaling. Based on these results, we propose that CDK9 inhibitors can potentiate the effects of immunotherapy against late-stage prostate cancer, a currently lethal disease.

2 | MATERIALS AND METHODS

2.1 | Cell lines and compounds

The LNCaP-MYC cell line is derived from the LNCaP model (from ATCC) and was described earlier.[21] LNCaP-MYC cells were maintained in RPMI medium supplemented with 10% fetal bovine serum (FBS) along with 200 μg/mL of Geneticin™ Selective Antibiotic (G418

Sulfate) and 2 μg/mL Puromycin. Overexpression of the MYC oncogene was achieved by the addition of doxycycline (2 μg/mL). C4-2 and 22RV1 cell lines were obtained from ATCC and maintained in RPMI medium supplemented with 10% FBS. For androgen-deprivation experiments, cells were kept in the phenol red-free RPMI medium supplemented with charcoal-stripped FBS (CSS) for three days. The following compounds were obtained from MedChemExpress: AT7519, Doxycycline, and PKR-IN-C16.

2.2 | Western blotting, lectin pulldown, and cell proliferation assays

For cell lysate preparation, we used the same method as previously described.[22] In brief, cells were washed with PBS, incubated in cell lysis buffer supplemented with proteinase, phosphatase and O-GlcNAcase (Thiamet G) inhibitors for 30 min, centrifuged at 15000 rpm for 5 min, and the supernatant was collected (all steps performed at +4°C). Protein concentration was determined with the bicinchoninic acid (BCA) assay. The following antibodies were used to detect the proteins of interest: from Santa Cruz Biotechnology: MAVS (sc-166 583), from Cell Signaling Technology: OGT (24083) and p-TBK1 (5483); and from Abcam: Actin (ab49900).

For lectin pulldown experiments, cells were androgen-deprived for three days, treated with 500 nM AT7519 for 4 h, and cell lysates prepared as for Western blotting. Agarose-bound succinylated wheat germ agglutinin (WGA) lectin (Vector Laboratories: AL-1023S) was used to enrich for glycosylated proteins as previously described,[23] agarose beads were used as controls, and samples were analyzed by Western blotting.

To measure cell viability, we used CellTiter-Glo 2.0 assays from Promega according to the manufacturer's instructions. All the viability data are from at least two biological replicates with three technical replicates each.

2.3 | Preparation of samples for SLAM-seq

LNCaP-MYC cells were depleted of androgens for two days. After this, cells were treated with 2 μg/mL doxycycline for 20 h. For the last 4 h, 500 nM AT7519 compound was added as indicated. Finally, for the last 10 min, 4-thiouridine was added. RNA isolation was performed using the Amersham RNAspin Mini Kit (Cytiva, catalog number: 25050071) according to the manufacturer's instructions. Part of the RNA was used in RT-qPCR to confirm the on-target effects (KLK3 primers: F-GCAGCATTGAACCAGAGGAG and R-AGAACTGGGGAGGCTTGAGT, and the other primers were obtained from previous reports: MYC and actin[24] and CLK3[15]). Purified RNA was alkylated as previously described.[25] Finally, library-preparation and sequencing were purchased as a service. In brief, libraries were prepared using QuantSeq 3′ mRNA-Seq library preparation (FWD) for Illumina sequencing, and sequencing was performed using SR100 High Throughput Sequencing on Illumina NextSeq 2000.

2.4 | Bioinformatics

SLAM-seq data analysis was performed using SLAM-DUNK,[26] which covers the entire pipeline from processing raw reads to achieving fully normalized quantification of nucleotide conversion. In this analysis, the identification of 4-thiouridine-labeled transcripts is based on the detection of T>C conversions. SLAM-DUNK produces two essential outputs: the raw counts of reads containing nucleotide conversions and a normalized estimation of labeled transcript fractions, accomplished through base-content and read coverage normalization. This enables one to obtain a comprehensive readout of the labeled transcripts. The differentially expressed genes from SLAM-seq and standard RNA-seq data were obtained using DESeq2.[27] To detect alternative splicing events, rMATS was used.[28] Gene set enrichment analysis was performed using the fgsea package in R. ChIP-seq data for p65 (the activating subunit of nuclear factor kappa-B [NFkB]) was obtained from GSE83860. In this experiment, the authors activated p65 by adding tumor necrosis factor alpha (TNFα) to LNCaP cells. We used MACS2[29,30] for peak calling. The differentially expressed genes, which were bound by p65 and whose expression changed in response to CDK9 inhibition, were found using Microsoft Excel. R (version 4.1.1) and R Studio (version 2023.03.0) were used to generate volcano-, box-, metagene-, and violin-plots.

2.5 | RT^2 Profiler PCR array

Innate immune transcriptional changes in LNCaP-MYC cells in response to treatment with AT7519, doxycycline, and combinations were measured using RT^2 Profiler PCR Array Human Antiviral Response (QIAGEN, 330231). Briefly, LNCaP-MYC cells were depleted of androgens for three days, followed by treatments for the next 72 h: 500 nM AT7519, 10 nM DHT, 2 μg/mL doxycycline, or combinations. RNA isolation was done using the Amersham RNAspin Mini Kit (Cytiva, catalog number: 25050071) and cDNA using the RT^2 First Strand Kit (Qiagen, 330401). cDNA was added to RT^2 SYBR Green Mastermix (Qiagen,

330522) and aliquoted to PCR arrays. Data were analyzed using an Excel-based data analysis template from Qiagen based on the ΔΔCT method with normalization of the raw data to housekeeping genes (*ACTB*, *B2M*, *GAPDH*, *HPRT1*, and *RPLPO*). All experiments were performed in biological duplicate.

2.6 | Knockdown and RT-qPCR of knockdown samples

An equal number of LNCaP-MYC cells were seeded on poly-L-lysine-coated 6-well plates for siRNA knockdown. Forward transfection was performed using Lipofectamine RNAiMAX Transfection Reagent in OPTI-MEM with 30 pmol of siRNA/well according to the manufacturer's instructions. After 24 h, the media was changed to charcoal-depleted FBS-containing media (androgen-deprived media) for 3 days prior to treatment with 500 nM AT7519 for 24 h. We obtained siRNAs from Thermo Fisher Scientific: Silencer™ Select Negative Control No. 1 siRNA catalog number: 4390843; EIF2AK2 (PKR) catalog number: 4390824, siRNA 1 assay ID: s11185 and siRNA 2 assay ID: s11186; and RELA catalog number: 4390824, siRNA 1 assay ID: s11915, siRNA 2 assay ID: s11916.

For RNA isolation, the cells were lysed in RLT Plus buffer and RNA isolated using the Qiagen RNeasy Plus Mini Kit (catalog no. 74134). cDNA Synthesis was achieved using qScript cDNA SuperMix (catalog no. 733–1177, Quantabio). Power SYBR™ Green PCR Master Mix (catalog no. 4367659, Applied Biosystems) was used to compare gene expression changes in PKR, RELA, and TNFα by real-time PCR (qPCR) in QuantStudio 5. Beta actin (ACTB) was used as the control. Primers for qPCR were purchased as follows: EIF2AK2 (CTGGTTCTTTTGCTACTACG and TCATAAGCAACGAAGAACTG) and RELA (GCAGAAAGAGGACATTGAG and GTGCACAT CAGCTTGC) from Sigma (KiCqStart predesigned); ACTB (TGGGACGACATGGAAAAT and AGAGGC GTACAGGGATAGCA) from Eurofins genomics; and human TNF-alpha from Stratech Scientific Ltd (sequence proprietary, catalog number: HP100592).

2.7 | Luminex cytokine analysis

LNCaP-MYC cells were depleted of androgens for three days, followed by treatment with 10 μg/mL doxycycline for 2 h. For the next 72 h, cells were treated with 500 nM AT7519, 2 μg/mL doxycycline, or combinations. After this, the conditioned media was collected for multiplex analysis using the Luminex MAGPIX® analyzer. We followed the sample preparation protocol provided by the manufacturer (Luminex), except the sample microparticle incubation was performed overnight at 4 degrees. Analyte concentrations were calculated based on the analyte standard curve and normalized to the total protein concentration in the cell lysate from the individual treatments. Protein concentration was determined by the Biorad protein assay reagent (5000006).

2.8 | ELISA

The conditioned media described above from LNCaP-MYC cells were also used for ELISA. Human IL-8 (Proteintech, KE00006) and CXCL10 (Proteintech, KE00128) sandwich ELISAs were performed according to the manufacturer's instructions, and absorbance readings were taken in a microplate reader at 450 and 630 nm. The cytokine levels were calculated based on standard curves. IL8 and CXCL10 levels were normalized to total protein.

3 | RESULTS

3.1 | CDK9 inhibition remodels the protein biosynthesis machinery

To emulate prostate cancer cell response to CDK9 inhibition in a clinically relevant experimental setting, we depleted prostate cancer cells of androgens and treated the cells with CDK9 inhibitor AT7519, a compound tested in clinical trials.[31,32] AT7519 treatment for 4 h decreased MYC mRNA by 75% but did not affect the expression levels of KLK3, a highly transcribed gene in prostate cancer cells (Figure 1A). These results imply some degree of gene-specificity arising from CDK9 inhibition, and we went on to assess this across the transcriptome.

We used metabolic labeling of RNA (SLAM-seq) to characterize how the short-term inhibition of CDK9 affects the nascent transcriptome in the absence of androgens (Figure 1B). In SLAM-seq, the newly synthesized RNA is labeled with 4-thiouridine, followed by chemical conversion of the label, which allows computational identification of the newly made mRNA.[25,26] As expected, transcription of the majority of the genes was downregulated when CDK9 was inhibited (Figure 1C). In addition, we noted that many genes were significantly more transcribed when we depleted CDK9 activity. These data show that the decline in CDK9 activity promotes the expression of a selective set of genes. Next, we focused on the set of genes induced by CDK9 inhibition.

SLAM-seq enables us to focus on the genes that are switched on/off at the given moment, and we wanted to better understand this response. We reasoned that the

genes selectively switched on when CDK9 is inhibited identify the processes that are important for cells to survive the imposed transcriptional stress. Based on the standard RNA-seq, most of the transcriptome was downregulated in response to AT7519 treatment in the same experimental setting (Figure S1). We labeled the nascent RNA for a very short time, only for the last 10 min of the inhibitor treatment (Figure 1B), which means that certain genes were actively transcribing even when CDK9 activity had been depleted for 4 h. By focusing on the genes that are induced based on the SLAM-seq but downregulated based on the RNA-seq at the same time-point, we can identify the genes that are initially downregulated but whose expression is rapidly restored after CDK9 inhibition (Figure 1D). We reasoned that these genes are critical to surviving the CDK9 inhibitor-induced stress. Next, we subjected the genes that are initially downregulated but whose expression is rapidly restored to pathway enrichment analysis using KEGG and Reactome.

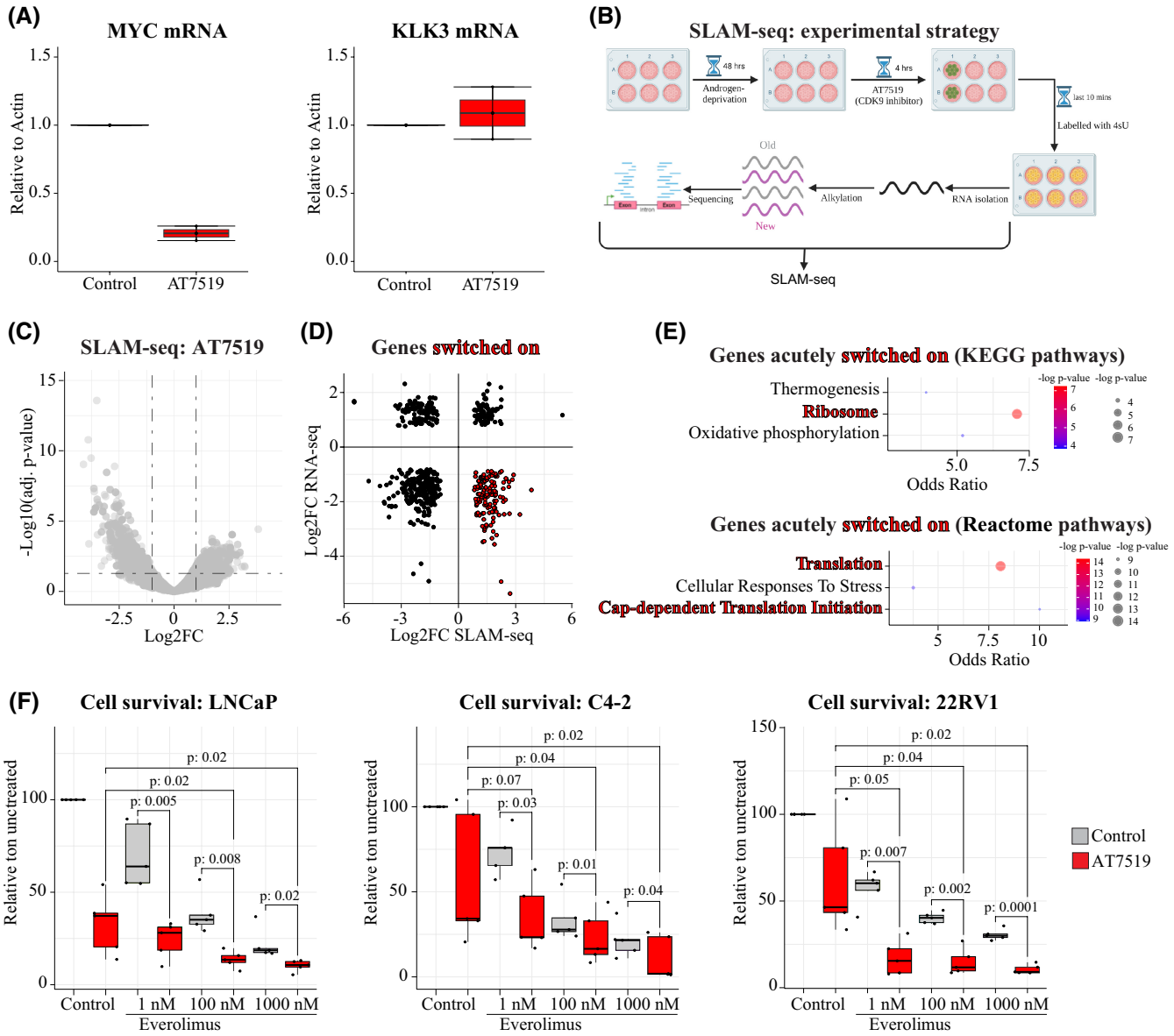

FIGURE 1 CDK9 inhibition remodels protein biosynthetic machinery. (A) RT-qPCR data analysis showing the on-target effect of CDK9 inhibition (500 nM AT7519 for 4 h) on MYC mRNA. The data represented are the average of two biological replicates with standard error of mean (SEM). (B) Graphical representation of the SLAM-seq experimental setup. (C) LNCaP-MYC cells were treated with 500 nM AT7519 for 4 h and analyzed using SLAM-DUNK. Data presented are significantly affected mRNAs ($p < .01$). (D) Genes highlighted in red were selected based on the following criteria: significantly ($p < .01$) upregulated in response to CDK9 inhibitor treatment in SLAM-seq and downregulated in RNA-seq. (E) Pathway enrichment analysis using Enrichr[33] performed on the selected set of genes from (D) (genes highlighted in red). (F) Cell viability was measured using CellTiter-Glo after 4 days of treatment with mTOR inhibitor (everolimus) in the presence or absence of AT7519 (LNCaP and C4-2: 0.5 μM; 22RV1: 2 μM). Data are from five biological replicates, each having three technical replicates.

This approach revealed that CDK9 inhibition induces genes related to protein biosynthesis machinery, in particular 'Ribosome', 'Translation', and 'Cap-dependent translation initiation' (Figure 1E).

We were curious if cells become more dependent on high levels of protein synthesis when CDK9 is inhibited. Global protein synthesis can be inhibited by targeting mTOR using Everolimus.[34,35] Combined inhibition of CDK9 and mTOR led to a complete loss of proliferation of prostate cancer and CRPC cells (Figure 1F). Together with the SLAM-seq data and increased sensitivity to mTOR inhibition, our results show that when CDK9 is inhibited, prostate cancer cells have a greater reliance on protein biosynthesis. It was unexpected to identify a high number of genes that were increasingly transcribed in response to CDK9 inhibition, and we moved on to better understand what these genes are.

3.2 | CDK9 inhibition transiently hyperactivates MYC signaling

We used gene set enrichment analysis (GSEA) to identify the biological processes activated when CDK9 is inhibited. MYC targets_V1 was among the most significantly induced gene sets (Figures 2A and S2). In addition, this approach identified 'Oxidative Phosphorylation' and 'Fatty Acid Metabolism' among the most significant pathways, in support of our previous findings showing that CDK9 inhibition induces remodeling of mitochondrial metabolism.[24,36] To validate this response, we repeated the GSEA using a previously generated RNA-seq dataset where the authors used the same CDK9 inhibitor in the presence of androgens.[9] Here, MYC targets_V1 was the most significantly upregulated response (Figures 2A and S2). MYC functions as a global amplifier of transcription,[37,38] and it is possible that the increased MYC signaling is part of the adaptive response to CDK9 inhibition. In support of this hypothesis, it has been established that CDK9 inhibition in melanoma and lung cancer cells leads to a rapid loss of the MYC mRNA, but within eight hours, the MYC expression is induced beyond the levels of the untreated cells.[39] We reasoned that increased MYC expression can rescue the cancer cells from CDK9 inhibitor-induced effects on transcription and moved on to directly probe this.

To further probe the crosstalk between CDK9 and MYC in the androgen-deprived prostate cancer cells, we performed a SLAM-seq experiment in the prostate cancer model, where MYC is induced by the addition of doxycycline (Figure 2B). By overexpressing MYC for 20 h before treating the cells with the CDK9 inhibitor, we restored the MYC mRNA close to that of the untreated cells (Figure 2C). More importantly, when MYC was first overexpressed for 20 h prior to treatment with the CDK9 inhibitor, the cells had almost twice higher MYC protein levels, which enabled us to probe the effects of MYC on the nascent transcription when CDK9 activity is depleted (Figure 2D). Next, we deprived prostate cancer cells of androgens for two days, induced MYC for 20 h, inhibited CDK9 for 4 h, and labeled the nascent transcription using 4sU for the last 10 min (Figure 2B). As expected, overexpression of MYC increased overall transcription based on the analysis of the nascent transcriptome and the total mRNA (Figure 2E). Strikingly, however, when we added CDK9 inhibitor to cells where MYC was overexpressed, we observed a further significant downregulation of both the active mRNA synthesis and the overall mRNA abundance when compared to CDK9 inhibition alone (Figure 2E).

We reasoned that hyperactivation of transcription due to MYC overexpression causes splicing defects when CDK9 is inhibited and thereby prevents the synthesis of mature mRNAs, which explains the further downregulation of transcription. We used rMATS[28] to identify the significant alternative splicing events under our experimental conditions. Indeed, CDK9 inhibition in cells with MYC overexpression caused the most severe splicing defects across the five major alternative splicing categories (Figure 2F). Previously, intron retention has been identified as a characterizing feature of aggressive prostate cancer,[16] which is why we validated splicing defects by focusing on the CLK3 retained intron, an mRNA known to be differently spliced when CDK9 is inhibited.[15] MYC overexpression combined with CDK9 inhibition further increased intron retention in the CLK3 mRNA compared to the single agent treatments (Figure S3).

It was unexpected that MYC overexpression prior to CDK9 inhibitor treatment further downregulates mRNA abundance compared to CDK9 inhibitor alone (Figure 2E). We propose that MYC overexpression enhances transcriptional processivity by stimulating transcription initiation, whilst CDK9 inhibition restricts transcription elongation. Collectively, this results in partially processed/complete transcripts akin to splicing defects; this is currently a hypothesis and can be probed using sensitive methods such as PRO-seq or TT-seq with multiple time points.[40] However, establishing this goes beyond the scope of the current manuscript to understand why prostate cancer cells are sensitive to CDK9 inhibition, and we next wanted to identify the factors that coordinate the altered activity of MYC and CDK9 to trigger the appropriate response.

3.3 | CDK9 inhibition induces glycosylation of the innate immune response factor MAVS

O-GlcNAc transferase (OGT) is found on transcriptionally active chromatin, and the enzyme coordinates with

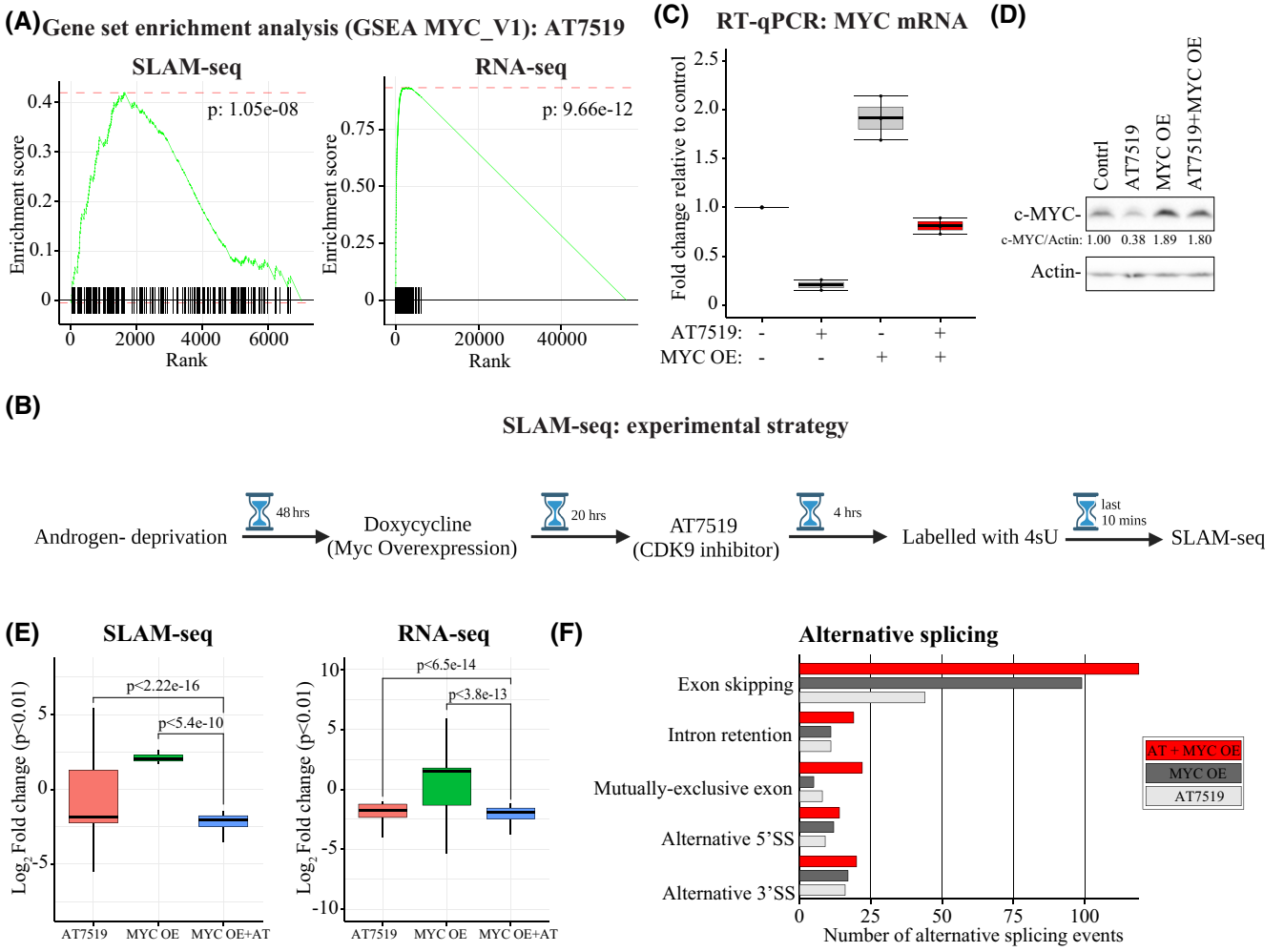

FIGURE 2 MYC overexpression augments CDK9 inhibitor-induced splicing defects. (A) GSEA enrichment plot for the MYC targets V1 Hallmark gene set for CDK9 inhibition (500 nM AT7519) affected genes after 4 h of treatment of LNCaP-MYC cells (SLAM-seq) and for LNCaP cells (RNA-seq; previously published data[9]). The X-axis shows the rank of the DEGs (calculated based on the $\log_2$ fold change and the p-value), and the Y-axis shows the enrichment scores. (B) SLAM-seq experimental setup: LNCaP-MYC cells were depleted of androgens for two days. After this, cells were treated with 2 μg/mL of doxycycline (MYC overexpression) for 20 h. For the last 4 h, 500 nM AT7519 (CDK9 inhibition) was added. Finally, for the last 10 min, 4-thiouridine was added. The experiment was performed in two biological replicates. (C) Confirmation of MYC overexpression (MYC OE) ± 500 nM CDK9 inhibitor (AT7519) using RT-qPCR (MYC OE for 20 h followed by CDK9 inhibitor treatment for 4 h). The data presented are the average of two biological replicates with an SEM. (D) Confirmation of MYC overexpression at the protein level (otherwise as in 2C). (E) Box plots indicating the effects of AT7519, MYC overexpression (MYC OE), and MYC OE + AT7519 on the expression levels of the genes analyzed by the SLAM-seq and RNA-seq pipelines. The significance of the difference between the treatments was evaluated using the Kruskall–Wallis test. (F) Significant alternative splicing (AS) events ($p < .05$ and FDR <0.05) in LNCaP-MYC cells treated with AT7519, MYC overexpression, and their combination (experimental setup as in (C)).

both MYC and CDK9 to regulate cell survival. High OGT activity is required for MYC-driven proliferation of prostate cancer cells,[41] and co-targeting of OGT and CDK9 is lethal to cancer cells.[9] OGT attaches a single sugar unit to the target proteins' serine and threonine residues, and its activity is selectively remodeled when CDK9 is inhibited.[42] To probe if OGT's target repertoire can explain the response to CDK9 inhibition, we used our previously published glycoproteome dataset.[42] In this experiment, CDK9 activity was depleted in LN95 cells using NVP2, a highly selective CDK9 inhibitor,[43] after which the glycoproteins were enriched using immunoprecipitation and the proteins were identified using mass spectrometry.[42] LN95 is an isogenic androgen-independent prostate cancer model derived from the LNCaP cells we used in most of the experiments in this study. We performed pathway enrichment analysis of the factors more glycosylated in response to CDK9 inhibition and identified the spliceosome as the most significantly affected process (Figure 3A). These data support the robust splicing defects we observed in response to CDK9 inhibition (Figure 2F).

We moved on to further explore the remodeling of the post-translational glycoprotein landscape in response to CDK9 inhibition with an unbiased approach. For this, we selected GeneWalk-tool, which makes use of deep learning and gene network-based topology information to identify the most important factors/regulators in the dataset.[44] This approach identified MAVS (mitochondrial antiviral signaling) as a hyper-glycosylated protein in response to CDK9 inhibition with the highly selective compound NVP2 (Figure 3B,C). Previously, it has been established that glycosylation of MAVS is essential to mounting an effective antiviral innate immune response.[45] We used lectin pulldown experiments to confirm that CDK9 inhibition with AT7519 also induces MAVS glycosylation (Figure 3D).

Our data so far show that CDK9 inhibition causes splicing defects that are enhanced when MYC is overexpressed. In addition, we show that CDK9 inhibition causes glycosylation of the innate immune response sensor MAVS. Previously, it has been established that MAVS glycosylation is required to activate the host's innate immune response against RNA viruses.[45] In an earlier study, Bowling et al. (2021) discovered that inhibition of the core spliceosome induces similar splicing defects in breast cancer cells,[11] as we observed here for CDK9 inhibition in prostate cancer cells. In the case of breast cancer, these splicing defects activate the signaling integrator MAVS, resulting in the initiation of an antiviral response.[11] We moved on to probe if inhibition of CDK9 activity could also activate this response.

3.4 | CDK9 inhibition activates innate immune-signaling through the dsRNA-sensor PKR

Accumulation of mis-spliced RNA and activation of MAVS can trigger an anti-viral innate immune response in a double-stranded RNA (dsRNA)-sensor-dependent manner in breast cancer cells.[11] One of the major dsRNA-sensors is protein kinase R (PKR), which can be directly inhibited through the small-molecule inhibitor PKR-IN-C16.[46] PKR-IN-C16 blocked the CDK9 inhibitor-induced anti-proliferative effects on prostate cancer and CRPC cells (Figure 4A,B). We have previously shown that CDK9 inhibition causes cancer cell-selective DNA damage,[42] which we reasoned also explains the anti-proliferative effects. In contrast to this, depleting PKR activity increased CDK9 inhibitor-induced DNA damage while rescuing the CDK9 inhibitor effects on viability (Figure 4A–C). These data propose that DNA damage itself is not the major cause of the CDK9 inhibitor-induced anti-proliferative effects on prostate cancer cells. Instead, we propose that the improperly processed RNA itself causes DNA damage. Accordingly, PKR inhibitor alone caused DNA damage and was highly toxic to prostate cancer cells over a longer time period (Figures 4C and S4). In interpreting these results, it is important to note that PKR functions as a context-dependent regulator, which can suppress DNA damage response signaling in cancer cells,[47] alleviate lipopolysaccharide-induced kidney toxicity by suppressing the production of

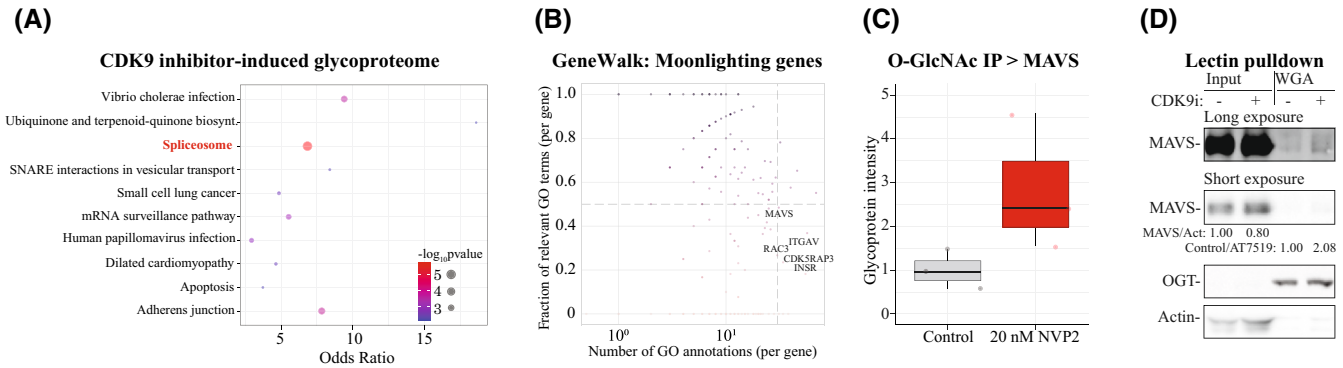

FIGURE 3 Innate immune response signaling factor MAVS is hyper-glycosylated in response to CDK9 inhibition. (A) Pathway enrichment analysis using Enrichr (Kyoto Encyclopedia of Genes and Genomes; KEGG). Genes were selected based on the following criteria: The protein was increasingly glycosylated by 20% in three biological replicates in response to CDK9 inhibitor NVP2 treatment of LN95 cells (20 nM NVP2; analysis of the previously published data[42]). (B) GeneWalk analysis of the proteins increasingly glycosylated in three biological replicates in response to CDK9 inhibitor NVP2 treatment of LN95 cells (analysis of the previously published data[42]). The lower and more right the gene is in the lowest right quadrant, the more likely it is that the gene performs multiple functions. (C) Glycoprotein signal intensity in the mass spectrometry data (n: 3 biological replicates). The values were first normalized to the negative immunoprecipitation sample and are presented here as relative to the untreated sample, which was set to a value of 1. (D) LNCaP cells were treated with a CDK9 inhibitor (500 nM AT7519) for 4 h, and wheat germ agglutinin (WGA)-lectin pulldown was used to enrich for proteins O-GlcNAcylated in the given conditions. The data are representative of two biological replicates; OGT is used as a positive control and actin as a negative control in the pulldown samples. For clarity, both long- and short-exposure Western blots of MAVS antibody are shown. Densitometry was used to determine the signal intensities.

pro-inflammatory cytokines,[48] and also regulate learning by affecting interferon-γ-mediated signaling in the central nervous system.[49] Nevertheless, cancer cells typically exhibit increased levels of transcription, and our data instill confidence in the hypothesis that the hyperactivated transcription leads to defects in splicing and the accumulation of mis-spliced mRNAs.

To directly establish if CDK9 inhibition activates the immune response, we performed targeted transcriptional profiling of 84 anti-viral innate immune response genes using RT-qPCR. Many of these genes are expressed at low levels, which is why we resorted to the targeted approach rather than using sequencing-based approaches. Strikingly, we noted 2–55-fold increase in the expression of 16 cytokines in response to CDK9 inhibition (Figure S5). Two of the most strongly stimulated cytokines were TNFα and CXCL10. To validate the importance of PKR for the CDK9 inhibitor-induced transcription of cytokine genes, we used two siRNAs to knockdown PKR and treated cells with the CDK9 inhibitor. This experiment revealed that depleting PKR from cells partially suppresses CDK9 inhibitor-induced expression of the *TNFα*-gene (Figure S6). To further connect CDK9 inhibitor-induced splicing defects to anti-viral signaling, we assessed if TANK-binding kinase 1 (TBK1) is activated in response to CDK9 inhibition. TBK1 functions as the major kinase in innate adaptor complexes, particularly in conjunction with MAVS, and it connects activation of the pattern recognition receptors to transcription factors, including NFkB, which then promotes the expression of the pro-inflammatory cytokines.[50] Indeed, CDK9 inhibition leads to a rapid activation of TBK1 (Figure S7). These data ascertain that CDK9 inhibition can induce immunogenic signaling, at least in part, through the same sensors used for viral sensing. At the same time, our experiment highlights that multiple sensors integrate information to activate the appropriate response, and depletion of a single factor fails to completely prevent this. However, depletion of the major regulator of the innate and adaptive immune responses, NFκB,[51] should prevent CDK9 inhibitor-induced activation of immunogenic transcription. To probe this, we first depleted the canonical NFκB subunit RELA using two distinct siRNAs and subsequently treated the cells with the CDK9 inhibitor. Indeed, depletion of RELA completely prevented CDK9 inhibitor-induced expression of TNFα (Figure 4D).

Our hypothesis is that CDK9 inhibition causes splicing defects, which in turn activate immunogenic signaling in prostate cancer cells due to the high levels of mis-spliced RNA. If this were the case, further stimulation of transcription due to MYC overexpression should burden the splicing machinery even more and thereby enhance immunogenic signaling. Indeed, MYC overexpression led to an even further increase in cytokine expression (Figure 4E).

We reasoned that CDK9 inhibition-induced activation of the protein biosynthetic machinery would lead to increased translation and subsequent secretion of the immunogenic cytokines, and this response should be further stimulated by MYC activation. For these experiments, we also selected IL8, which is known to be overexpressed in prostate cancer cells.[52] CDK9 inhibition induced a significant 10-fold increase in the secretion of TNFα, CXCL10, and IL8, as determined using FACS-based Luminex multiplex cytokine analysis (Figure 4F). Strikingly, overexpression of MYC doubled the amount of CDK9 inhibitor-induced secretion of TNFα, CXCL10, and IL8 (Figure 4F). The combinatorial effects of MYC overexpression and CDK9 inhibition on the secreted TNFα were robust; however, the effects on CXCL10 and IL8 were modest, which is why we confirmed these using ELISA (Figure S8).

These data demonstrate that CDK9 inhibition induces a response similar to viral infection/innate immune response, which can be further augmented when transcription is hyperactivated due to MYC overexpression. Next, we wanted to better understand the crosstalk between TNFα-signaling and CDK9 inhibition-induced transcriptional effects.

3.5 | CDK9 inhibition allows selective signaling through NFκB

In response to viral infection, accumulation of the dsRNA leads to a decrease in the host's transcription, yet some genes are expressed and translated to mount the appropriate response to fight the infection.[53] Based on our results so far, CDK9 inhibition suppresses transcription of most genes but allows transcription of immunogenic cytokines. We identified the master regulator of innate and adaptive immune responses, NFκB,[51] as a necessary factor to activate the expression of the TNFα-gene in response to CDK9 inhibition (Figure 4D). We also confirmed that TNFα is secreted in response to CDK9 inhibition (Figure 4F). TNFα is one of the main activators of NFκB,[54] and we therefore reasoned that CDK9 inhibition activates a feed-forward loop by selectively stimulating transcription of the NFκB target genes. This transcription program may be active in prostate cancer patient tumors, which suffer from appropriate transcriptional stress. We moved on to formally test this.

To identify NFκB binding sites in our prostate cancer model, we used a previously published ChIP-seq dataset against the active subunit of NFκB, RELA; this dataset was generated in the LNCaP cell line.[55] Next, we assessed

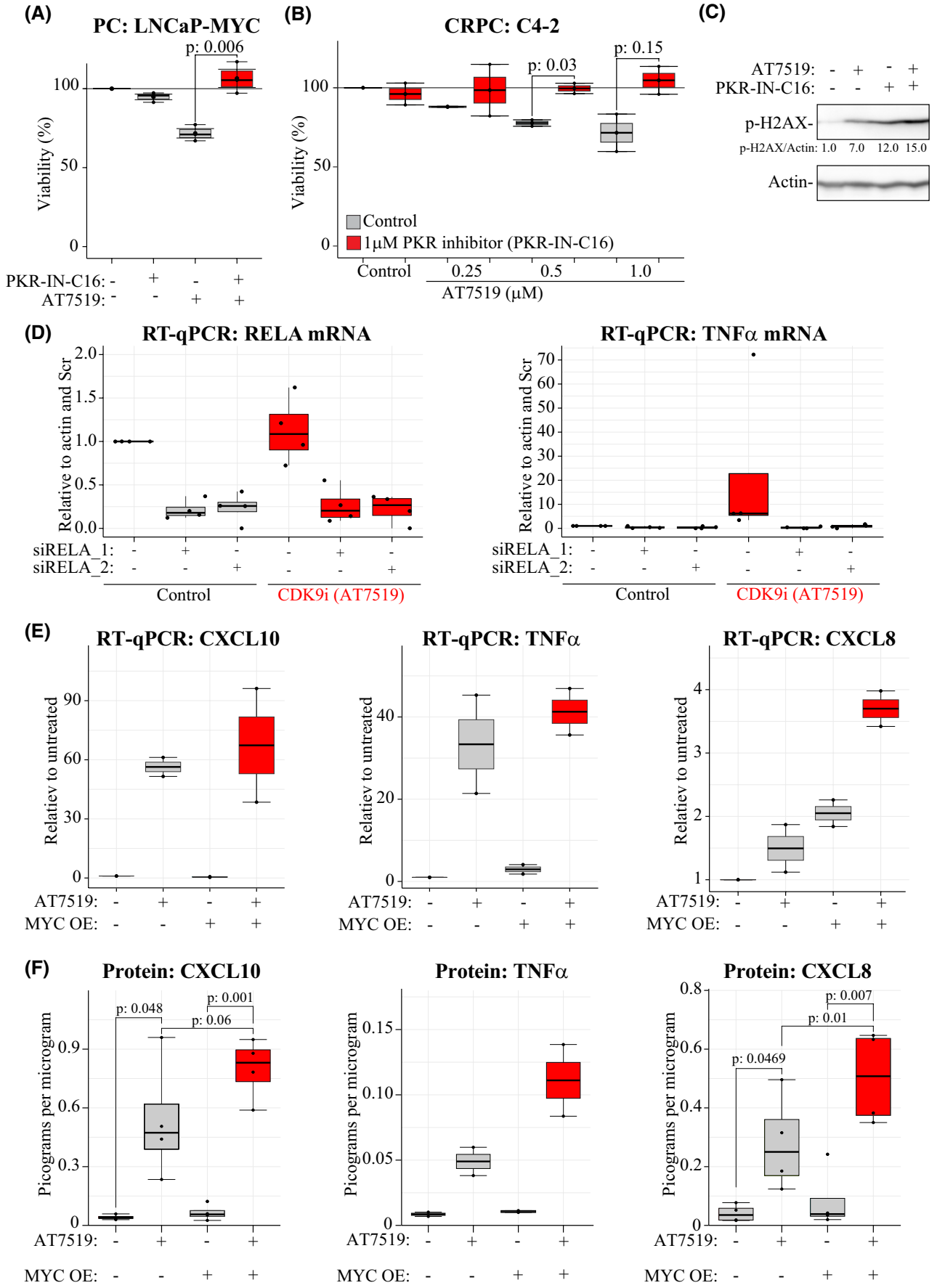
(A)
PC: LNCaP-MYC
p: 0.006
Viability (%)
100
50
0
PKR-IN-C16: - + - +
AT7519: - - + +
(B)
CRPC: C4-2
p: 0.03
p: 0.15
Viability (%)
100
50
0
Control
1μM PKR inhibitor (PKR-IN-C16)
Control 0.25 0.5 1.0
AT7519 (μM)
(C)
AT7519: - + - +
PKR-IN-C16: - - + +
p-H2AX-
p-H2AX/Actin: 1.0 7.0 12.0 15.0
Actin-
(D)
RT-qPCR: RELA mRNA
Relative to actin and Scr
2.0
1.5
1.0
0.5
0.0
siRELA_1: - + - - + -
siRELA_2: - - + - - +
Control
CDK9i (AT7519)
RT-qPCR: TNFα mRNA
Relative to actin and Scr
70
60
50
40
30
20
10
0
siRELA_1: - + - - + -
siRELA_2: - - + - - +
Control
CDK9i (AT7519)
(E)
RT-qPCR: CXCL10
Relatiev to untreated
90
60
30
0
AT7519: - + - +
MYC OE: - - + +
RT-qPCR: TNFα
Relatiev to untreated
40
20
0
AT7519: - + - +
MYC OE: - - + +
RT-qPCR: CXCL8
Relatiev to untreated
4
3
2
1
AT7519: - + - +
MYC OE: - - + +
(F)
Protein: CXCL10
p: 0.048
p: 0.001
p: 0.06
Picograms per microgram
0.9
0.6
0.3
0
AT7519: - + - +
MYC OE: - - + +
Protein: TNFα
Picograms per microgram
0.15
0.10
0.05
0
AT7519: - + - +
MYC OE: - - + +
Protein: CXCL8
p: 0.007
p: 0.01
p: 0.0469
Picograms per microgram
0.8
0.6
0.4
0.2
0
AT7519: - + - +
MYC OE: - - + +

FIGURE 4 MYC overexpression augments CDK9 inhibitor-activated immunogenic signaling. (A) LNCaP-MYC cells were treated for 24 h with 500 nM AT7519, either in the presence or absence of 1 μM PKR inhibitor PKR-IN-C16. Two-tailed paired samples Student's *t*-test was used to assess the statistical significance. The data presented are the average of three biological replicates with an SEM. (B) C4-2 cells were treated for 24 h with different doses of AT7519 alone or in combination with a 1 μM PKR inhibitor, and a cell viability assay was performed. Replicates and significance are as in (A). (C) LNCaP-MYC cells were treated as indicated (time-points/doses as in (A)) and analyzed using Western blot. Densitometry was used to quantitate the signal intensity. (D) Knockdown of the NFκB subunit RELA prevents CDK9 inhibitor-induced expression of the TNFα-gene (n: 3–4 biological replicates). (E) Box plots showing the selected mRNAs from the RT^2 Profiler PCR Array Human Antiviral Response-Array experiment from Figure S5. (F) Analysis of the secreted cytokines from cell culture media. LNCaP-MYC cells were depleted of androgens for three days. For the next 72 h, cells were treated with 500 nM AT7519, 2 μg/mL doxycycline, or combinations, and conditioned media were collected for Luminex multiplex cytokine analysis. Statistical analysis performed as in (A). The data presented for CXCL10 and IL8 are the average of four biological replicates, and for TNFα, they are of two biological replicates with a standard deviation.

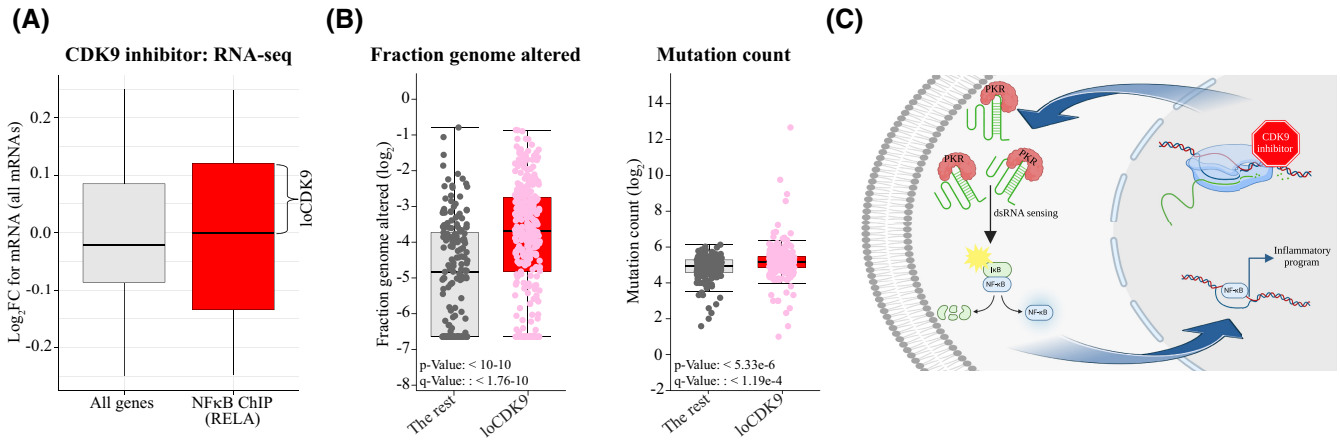

FIGURE 5 Identification of a gene signature predictive of genome instability. (A) Box plot of CDK9 inhibitor-affected mRNAs after treatment of LNCaP cells with 500 nM AT7519 (analysis of previously published data (GSE169090[9])). NFκB binding sites were identified from a previously published dataset generated from the same cell line (GSE83860).[55] (B) Box plot depicting the high genome instability and high mutation count of the tumors exhibiting altered expression of the loCDK9 gene signature (TCGA prostate adenocarcinoma dataset). The plot was generated using the data available in cBioPortal. (C) Graphical summary of CDK9 inhibition-induced immunogenic signaling. CDK9 inhibition causes splicing defects, which activate double-stranded RNA-activated kinase (PKR). PKR promotes the release of NFκB to the nucleus, which activates transcription of a selective subset of the inflammatory genes, and CDK9 inhibitor-induced protein synthesis allows their efficient translation.

how CDK9 inhibition affects transcription of the genes bound by RELA using the RNA-seq data of LNCaP cells treated with the CDK9 inhibitor AT7519. Indeed, a subset of the NFκB target genes was increased in response to CDK9 inhibition (Figure 5A).

We termed the identified group of genes the 'loCDK9-signature' and used this signature to stratify prostate cancer patients based on their clinical features. The loCDK9-signature is the gene bound by p65 and overexpressed in response to 500 nM AT7519 (Figure 5A). The loCDK9-signature identified prostate cancer patients with extensive genome instability in their tumors (Figure 5B). Earlier, we noted that CDK9 inhibition induces robust DNA damage (Figure 4C). Genome instability is the best-understood feature predicting response to immunotherapy.[56,57] We hypothesize that CDK9 inhibition can be used to induce DNA damage in prostate cancer cells that show high levels of transcription due to hyperactivation of oncogenic transcription factors, in particular c-MYC.

In summary, here we show that CDK9 inhibition can be used to activate the inflammatory response in prostate cancer cells (Figure 5C). Our data propose that compounds targeting CDK9 could be used as adjuvants for targeted immunotherapy.

4 | DISCUSSION

Prostate cancer is prevalent among males, and there is a necessity to develop an effective therapeutic strategy against this disease. The current treatment against

prostate cancer, anti-androgen therapy, often leads to the development of resistance, which establishes a need for alternative therapeutic approaches. In this study, we investigated targeting CDK9, a key regulator of transcription elongation, as a therapeutic strategy against prostate cancer. We show that CDK9 inhibition causes greater dependence on high levels of protein synthesis. This occurs primarily through mTORC1 signaling based on gene set enrichment analysis of our SLAM-seq data and increased sensitivity to mTOR inhibitor Everolimus (Figures 1E,F and S2). Stimulation of protein biosynthesis enables cells to stabilize the proteome in a situation where the overall transcription is downregulated.

Our findings revealed that CDK9 inhibition leads to downregulation of the majority of mRNAs in prostate cancer cells (Figure 1D), consistent with the well-established role of CDK9 in promoting transcription elongation.[12] Unexpectedly, we discovered that CDK9 inhibition induced MYC signaling, despite the decrease in MYC mRNA and protein levels (Figure 2A,C,D). We propose that this represents an adaptive mechanism, which we then moved on to probe further.

To further understand the effects of CDK9 inhibition on MYC overexpressing prostate cancer cells, we examined its impact on alternative splicing. Our laboratory discovered that CDK9 inhibition causes significant alternative splicing,[15] particularly intron retention, which has been identified by others as a characteristic feature of aggressive prostate cancer.[16] We hypothesized that MYC overexpression-induced hyperactivation of transcription would augment the splicing defects induced by CDK9 inhibition. Indeed, MYC overexpression increased CDK9 inhibitor-induced splicing defects, including intron retention in the CLK3 mRNA (Figures 2F and S3). In future studies, it is important to establish mechanistically how MYC overexpression augments CDK9 inhibitor-induced splicing defects. This can be probed, for example, by purifying RNA Pol II from cells where MYC is overexpressed and CDK9 activity is depleted and characterizing the associated proteome using mass spectrometry.

In addition to splicing defects, our study further explored post-translational remodeling of the glycoproteome in response to CDK9 inhibition. Pathway-enrichment analysis of the glycoproteome data identified the spliceosome as the most significant process affected in response to CDK9 inhibition (Figure 3A). Strikingly, by using an unbiased approach, we discovered that CDK9 inhibition induces glycosylation of the MAVS protein (Mitochondrial Antiviral Signaling; Figure 3B). Glycosylation of MAVS is required for mounting an effective antiviral innate immune response.[45] These data propose that defects in splicing, particularly increased intron retention, can activate the antiviral innate immune response due to the accumulation of improperly processed double-stranded RNA (dsRNA). To confirm this, we show that depletion of the dsRNA-activated PKR activity prevents CDK9 inhibitor-induced antiproliferative effects (Figure 4A,B). Our data indicate that CDK9 inhibition-induced effects mimic viral infection, leading to the activation of antiviral signaling. Indeed, CDK9 inhibition triggered the secretion of pro-inflammatory cytokines (Figure 4F). To relate the CDK9 inhibitor-induced splicing defects to viral sensing, we used a knockdown strategy to first deplete either PKR or NFkB activities, which revealed that both of these factors contribute to the CDK9 inhibitor-induced expression of the TNFα-gene (Figures 4D and S6).

We moved on to better understand if the genes differentially expressed in response to CDK9 inhibition identify a specific set of prostate cancer patients. Because we noted a response similar to anti-viral signaling in response to CDK9 inhibition, we reasoned that a specific set of genes are induced when CDK9 activity is impaired. To identify these genes, we looked for the genes that are regulated by NFκB, one of the major regulators of the inflammatory response.[58,59] Using this approach, we developed a loCDK9-signature, which identified patients with extensive genome instability (Figure 5A,B), one of the best predictive biomarkers for a good response to immunotherapy.[60,61] Earlier, it was established that CDK9 inhibition induces DNA damage in prostate cancer cells but not in normal prostate cells.[42] Both the splicing defects and the increase in genomic instability should enhance the immunogenicity of prostate cancer cells; this must be confirmed in future studies using syngeneic mouse models.

In conclusion, here we show that CDK9 inhibition overwhelms the spliceosome in cancer cells with high levels of transcription, which these cells interpret as a viral infection and go on to activate the innate immune response. Our data show that targeting CDK9 activates immunogenic signaling, and we thereby identify a novel treatment strategy to 'heat' the immunologically cold prostate tumors. In the future, it is important to establish if CDK9 inhibitors can potentiate the effects of immunotherapy against late-stage prostate cancer, a currently lethal disease.

AUTHOR CONTRIBUTIONS

SY analyzed the SLAM-seq data, performed the viability assays, prepared all the figures, and developed the manuscript drafts. AG prepared the samples for the SLAM-seq experiment and for cytokine mRNA profiling. NP performed the RT^2 Profiler PCR Array, Luminex multiplex cytokine analysis, and ELISA. JL performed the GeneWalk analysis. IGM supported the development of the project

and provided critical feedback. HMI conceptualized the project, obtained resources, supervised experiments, and wrote the manuscript. All authors read and approved the final manuscript.

ACKNOWLEDGMENTS

The authors wish to acknowledge CSC – IT Center for Science, Finland, for the computational resources. SY was funded in part by the EDUFI Fellowship. AG is supported in part by The Magnus Ehrnrooth Foundation. NP is funded by the Rosetrees Trust (PGL21/10171). JL was supported for a part of this project by funding from the Maud Kuistila Memorial Foundation. IGM is funded by the John Black Charitable Foundation, the Rosetrees Trust (Seedcorn2021/100216), and Prostate Cancer UK. HMI is grateful for the funding from the Academy of Finland (Decision nrs. 331324, 358112 and 335902), the Jenny and Antti Wihuri Foundation, the Sigrid Juselius Foundation, Rosetrees Trust (Seedcorn2021/100216), and EDUFI (Finnish National Agency for Education). The funders had no role in the conceptualization, design, data collection, analysis, decision to publish, or preparation of the manuscript.

DISCLOSURES

The authors declare no conflicts of interest.

DATA AVAILABILITY STATEMENT

The data generated or analyzed during this study are included in this manuscript and its supplementary information files. In addition, the sequencing data are deposited in the GEO database under the identifier 'GSE246384'.

ORCID

Shivani Yalala https://orcid.org/0009-0007-6105-8563
Aishwarya Gondane https://orcid.org/0000-0002-7495-2472
Ninu Poulose https://orcid.org/0000-0003-4578-6046
Jing Liang https://orcid.org/0009-0003-2513-6764
Ian G. Mills https://orcid.org/0000-0001-5347-5083
Harri M. Itkonen https://orcid.org/0000-0002-5194-7064

REFERENCES

1. Siegel RL, Miller KD, Fuchs HE, Jemal A. Cancer statistics, 2021. *CA Cancer J Clin*. 2021;71(1):7-33. doi:10.3322/caac.21654
2. Sandhu S, Moore CM, Chiong E, Beltran H, Bristow RG, Williams SG. Prostate cancer. *Lancet*. 2021;398(10305):1075-1109. doi:10.1016/S0140-6736(21)00950-8
3. Kelly RW. Immunosuppressive mechanisms in semen: implications for contraception. *Hum Reprod*. 1995;10(7):1686-1693. doi:10.1093/oxfordjournals.humrep.a136156
4. Lai JJ, Lai KP, Zeng W, Chuang KH, Altuwaijri S, Chang C. Androgen receptor influences on body defense system via modulation of innate and adaptive immune systems: lessons from conditional AR knockout mice. *Am J Pathol*. 2012;181(5):1504-1512. doi:10.1016/j.ajpath.2012.07.008
5. Ben-Batalla I, Vargas-Delgado ME, von Amsberg G, Janning M, Loges S. Influence of androgens on immunity to self and foreign: effects on immunity and cancer. *Front Immunol*. 2020;11:1184. doi:10.3389/fimmu.2020.01184
6. Sharma NL, Massie CE, Ramos-Montoya A, et al. The androgen receptor induces a distinct transcriptional program in castration-resistant prostate cancer in man. *Cancer Cell*. 2013;23(1):35-47. doi:10.1016/j.ccr.2012.11.010
7. Bou-Dargham MJ, Sha L, Sang QA, Zhang J. Immune landscape of human prostate cancer: immune evasion mechanisms and biomarkers for personalized immunotherapy. *BMC Cancer*. 2020;20(1):572. doi:10.1186/s12885-020-07058-y
8. Boutz PL, Bhutkar A, Sharp PA. Detained introns are a novel, widespread class of post-transcriptionally spliced introns. *Genes Dev*. 2015;29(1):63-80. doi:10.1101/gad.247361.114
9. Itkonen HM, Poulose N, Steele RE, et al. Inhibition of O-GlcNAc transferase renders prostate cancer cells dependent on CDK9. *Mol Cancer Res*. 2020;18(10)1512-1521. doi:10.1158/1541-7786.MCR-20-0339
10. Martin SES, Tan ZW, Itkonen HM, et al. Structure-based evolution of low Nanomolar O-GlcNAc transferase inhibitors. *J Am Chem Soc*. 2018;140(42):13542-13545. doi:10.1021/jacs.8b07328
11. Bowling EA, Wang JH, Gong F, et al. Spliceosome-targeted therapies trigger an antiviral immune response in triple-negative breast cancer. *Cell*. 2021;184(2):384-403.e321. doi:10.1016/j.cell.2020.12.031
12. Chou J, Quigley DA, Robinson TM, Feng FY, Ashworth A. Transcription-associated cyclin-dependent kinases as targets and biomarkers for cancer therapy. *Cancer Discov*. 2020;10(3):351-370. doi:10.1158/2159-8290.CD-19-0528
13. Marasco LE, Kornblihtt AR. The physiology of alternative splicing. *Nat Rev Mol Cell Biol*. 2023;24(4):242-254. doi:10.1038/s41580-022-00545-z
14. Mandal R, Becker S, Strebhardt K. Targeting CDK9 for anti-cancer therapeutics. *Cancers (Basel)*. 2021;13(9):2181. doi:10.3390/cancers13092181
15. Hu Q, Poulose N, Girmay S, et al. Inhibition of CDK9 activity compromises global splicing in prostate cancer cells. *RNA Biol*. 2021;18(sup2):722-729. doi:10.1080/15476286.2021.1983287
16. Zhang D, Hu Q, Liu X, et al. Intron retention is a hallmark and spliceosome represents a therapeutic vulnerability in aggressive prostate cancer. *Nat Commun*. 2020;11(1):2089. doi:10.1038/s41467-020-15815-7
17. Phillips JW, Pan Y, Tsai BL, et al. Pathway-guided analysis identifies Myc-dependent alternative pre-mRNA splicing in aggressive prostate cancers. *Proc Natl Acad Sci USA*. 2020;117(10):5269-5279. doi:10.1073/pnas.1915975117
18. Rasool RU, Natesan R, Deng Q, et al. CDK7 inhibition suppresses castration-resistant prostate cancer through MED1 inactivation. *Cancer Discov*. 2019;9(11):1538-1555. doi:10.1158/2159-8290.CD-19-0189
19. Liu H, Liu K, Dong Z. Targeting CDK12 for cancer therapy: function, mechanism, and drug discovery. *Cancer Res*. 2021;81(1):18-26. doi:10.1158/0008-5472.CAN-20-2245

20. Lam LT, Pickeral OK, Peng AC, et al. Genomic-scale measurement of mRNA turnover and the mechanisms of action of the anti-cancer drug flavopiridol. *Genome Biol*. 2001;2(10):RESEARCH0041. doi:10.1186/gb-2001-2-10-research0041
21. Ramos-Montoya A, Lamb AD, Russell R, et al. HES6 drives a critical AR transcriptional programme to induce castration-resistant prostate cancer through activation of an E2F1-mediated cell cycle network. *EMBO Mol Med*. 2014;6(5):651-661. doi:10.1002/emmm.201303581
22. Itkonen HM, Minner S, Guldvik IJ, et al. O-GlcNAc transferase integrates metabolic pathways to regulate the stability of c-MYC in human prostate cancer cells. *Cancer Res*. 2013;73(16):5277-5287. doi:10.1158/0008-5472.CAN-13-0549
23. Itkonen HM, Mills IG. Studying N-linked glycosylation of receptor tyrosine kinases. *Methods Mol Biol*. 2015;1233:103-109. doi:10.1007/978-1-4939-1789-1_10
24. Itkonen HM, Poulose N, Walker S, Mills IG. CDK9 inhibition induces a metabolic switch that renders prostate cancer cells dependent on fatty acid oxidation. *Neoplasia*. 2019;21(7):713-720. doi:10.1016/j.neo.2019.05.001
25. Herzog VA, Reichholf B, Neumann T, et al. Thiol-linked alkylation of RNA to assess expression dynamics. *Nat Methods*. 2017;14(12):1198-1204. doi:10.1038/nmeth.4435
26. Neumann T, Herzog VA, Muhar M, et al. Quantification of experimentally induced nucleotide conversions in high-throughput sequencing datasets. *BMC Bioinformatics*. 2019;20(1):258. doi:10.1186/s12859-019-2849-7
27. Love MI, Huber W, Anders S. Moderated estimation of fold change and dispersion for RNA-seq data with DESeq2. *Genome Biol*. 2014;15(12):550. doi:10.1186/s13059-014-0550-8
28. Shen S, Park JW, Lu ZX, et al. rMATS: robust and flexible detection of differential alternative splicing from replicate RNA-Seq data. *Proc Natl Acad Sci USA*. 2014;111(51):E5593-E5601. doi:10.1073/pnas.1419161111
29. Liu T. Use model-based analysis of ChIP-Seq (MACS) to analyze short reads generated by sequencing protein-DNA interactions in embryonic stem cells. *Methods Mol Biol*. 2014;1150:81-95. doi:10.1007/978-1-4939-0512-6_4
30. Zhang Y, Liu T, Meyer CA, et al. Model-based analysis of ChIP-Seq (MACS). *Genome Biol*. 2008;9(9):R137. doi:10.1186/gb-2008-9-9-r137
31. Chen EX, Hotte S, Hirte H, et al. A phase I study of cyclin-dependent kinase inhibitor, AT7519, in patients with advanced cancer: NCIC clinical trials group IND 177. *Br J Cancer*. 2014;111(12):2262-2267. doi:10.1038/bjc.2014.565
32. Mahadevan D, Plummer R, Squires MS, et al. A phase I pharmacokinetic and pharmacodynamic study of AT7519, a cyclin-dependent kinase inhibitor in patients with refractory solid tumors. *Ann Oncol*. 2011;22(9):2137-2143. doi:10.1093/annonc/mdq734
33. Chen EY, Tan CM, Kou Y, et al. Enrichr: interactive and collaborative HTML5 gene list enrichment analysis tool. *BMC Bioinformatics*. 2013;14:128. doi:10.1186/1471-2105-14-128
34. Liu GY, Sabatini DM. mTOR at the nexus of nutrition, growth, ageing and disease. *Nat Rev Mol Cell Biol*. 2020;21(4):183-203. doi:10.1038/s41580-019-0199-y
35. Saran U, Foti M, Dufour JF. Cellular and molecular effects of the mTOR inhibitor everolimus. *Clin Sci (Lond)*. 2015;129(10):895-914. doi:10.1042/CS20150149
36. Gondane A, Poulose N, Walker S, Mills IG, Itkonen HM. O-GlcNAc transferase maintains metabolic homeostasis in response to CDK9 inhibition. *Glycobiology*. 2022;32(9):751-759. doi:10.1093/glycob/cwac038
37. Lin CY, Loven J, Rahl PB, et al. Transcriptional amplification in tumor cells with elevated c-Myc. *Cell*. 2012;151(1):56-67. doi:10.1016/j.cell.2012.08.026
38. Nie Z, Guo C, Das SK, et al. Dissecting transcriptional amplification by MYC. *Elife*. 2020;9:e52483. doi:10.7554/eLife.52483
39. Lu H, Xue Y, Yu GK, et al. Compensatory induction of MYC expression by sustained CDK9 inhibition via a BRD4-dependent mechanism. *elife*. 2015;4:e06535. doi:10.7554/eLife.06535
40. Gondane A, Itkonen HM. Revealing the history and mystery of RNA-Seq. *Curr Issues Mol Biol*. 2023;45(3):1860-1874. doi:10.3390/cimb45030120
41. Itkonen HM, Urbanucci A, Martin SE, et al. High OGT activity is essential for MYC-driven proliferation of prostate cancer cells. *Theranostics*. 2019;9(8):2183-2197. doi:10.7150/thno.30834
42. Gondane A, Girmay S, Heleva A, Pallasaho S, Loda M, Itkonen HM. O-GlcNAc transferase couples MRE11 to transcriptionally active chromatin to suppress DNA damage. *J Biomed Sci*. 2022;29(1):13. doi:10.1186/s12929-022-00795-1
43. Olson CM, Jiang B, Erb MA, et al. Pharmacological perturbation of CDK9 using selective CDK9 inhibition or degradation. *Nat Chem Biol*. 2018;14(2):163-170. doi:10.1038/nchembio.2538
44. Ietswaart R, Gyori BM, Bachman JA, Sorger PK, Churchman LS. GeneWalk identifies relevant gene functions for a biological context using network representation learning. *Genome Biol*. 2021;22(1):55. doi:10.1186/s13059-021-02264-8
45. Song N, Qi Q, Cao R, et al. MAVS O-GlcNAcylation is essential for host antiviral immunity against lethal RNA viruses. *Cell Rep*. 2019;28(9):2386-2396.e2385. doi:10.1016/j.celrep.2019.07.085
46. Jammi NV, Whitby LR, Beal PA. Small molecule inhibitors of the RNA-dependent protein kinase. *Biochem Biophys Res Commun*. 2003;308(1):50-57. doi:10.1016/s0006-291x(03)01318-4
47. Cheng X, Byrne M, Brown KD, et al. PKR inhibits the DNA damage response, and is associated with poor survival in AML and accelerated leukemia in NHD13 mice. *Blood*. 2015;126(13):1585-1594. doi:10.1182/blood-2015-03-635227
48. Zhou J, Zhang F, Lin H, et al. The protein kinase R inhibitor C16 alleviates sepsis-induced acute kidney injury through modulation of the NF-kappaB and NLR family pyrin domain-containing 3 (NLPR3) pyroptosis signal pathways. *Med Sci Monit*. 2020;26:e926254. doi:10.12659/MSM.926254
49. Zhu PJ, Huang W, Kalikulov D, et al. Suppression of PKR promotes network excitability and enhanced cognition by interferon-gamma-mediated disinhibition. *Cell*. 2011;147(6):1384-1396. doi:10.1016/j.cell.2011.11.029
50. Zhou R, Zhang Q, Xu P. TBK1, a central kinase in innate immune sensing of nucleic acids and beyond. *Acta Biochim Biophys Sin Shanghai*. 2020;52(7):757-767. doi:10.1093/abbs/gmaa051
51. Liu T, Zhang L, Joo D, Sun SC. NF-kappaB signaling in inflammation. *Signal Transduct Target Ther*. 2017;2:17023. doi:10.1038/sigtrans.2017.23
52. Madan RA, Palena C. Behind the IL-8 ball in prostate cancer. *Nat Can*. 2021;2(8):775-776. doi:10.1038/s43018-021-00235-3

53. Chen YG, Hur S. Cellular origins of dsRNA, their recognition and consequences. *Nat Rev Mol Cell Biol*. 2022;23(4):286-301. doi:10.1038/s41580-021-00430-1
54. Guo Q, Jin Y, Chen X, et al. NF-kappaB in biology and targeted therapy: new insights and translational implications. *Signal Transduct Target Ther*. 2024;9(1):53. doi:10.1038/s41392-024-01757-9
55. Malinen M, Niskanen EA, Kaikkonen MU, Palvimo JJ. Crosstalk between androgen and pro-inflammatory signaling remodels androgen receptor and NF-kappaB cistrome to reprogram the prostate cancer cell transcriptome. *Nucleic Acids Res*. 2017;45(2):619-630. doi:10.1093/nar/gkw855
56. Chen M, Linstra R, van Vugt M. Genomic instability, inflammatory signaling and response to cancer immunotherapy. *Biochim Biophys Acta Rev Cancer*. 2022;1877(1):188661. doi:10.1016/j.bbcan.2021.188661
57. Mardis ER. Neoantigens and genome instability: impact on immunogenomic phenotypes and immunotherapy response. *Genome Med*. 2019;11(1):71. doi:10.1186/s13073-019-0684-0
58. Li Q, Verma IM. NF-kappaB regulation in the immune system. *Nat Rev Immunol*. 2002;2(10):725-734. doi:10.1038/nri910
59. van Loo G, Bertrand MJM. Death by TNF: a road to inflammation. *Nat Rev Immunol*. 2023;23(5):289-303. doi:10.1038/s41577-022-00792-3
60. Marabelle A, Fakih M, Lopez J, et al. Association of tumour mutational burden with outcomes in patients with advanced solid tumours treated with pembrolizumab: prospective biomarker analysis of the multicohort, open-label, phase 2 KEYNOTE-158 study. *Lancet Oncol*. 2020;21(10):1353-1365. doi:10.1016/S1470-2045(20)30445-9
61. Pilard C, Ancion M, Delvenne P, Jerusalem G, Hubert P, Herfs M. Cancer immunotherapy: it's time to better predict patients' response. *Br J Cancer*. 2021;125(7):927-938. doi:10.1038/s41416-021-01413-x

SUPPORTING INFORMATION

Additional supporting information can be found online in the Supporting Information section at the end of this article.

How to cite this article: Yalala S, Gondane A, Poulose N, Liang J, Mills IG, Itkonen HM. CDK9 inhibition activates innate immune response through viral mimicry. *The FASEB Journal*. 2024;38:e23628. doi:10.1096/fj.202302375R